Homan, R., & Pownall, H. J. (1988) *Biochim. Biophys. Acta 938*, 155-166.
Hutton, W. C., Yeagle, P. L., & Martin, R. B. (1977) *Chem. Phys. Lipids 19*, 255-265.
Janatova, J., Fuller, J. K., & Hunter, M. J. (1968) *J. Biol. Chem. 243*, 3612-3622.
Kawaguchi, A., Yoshimura, T., & Okuda, S. (1981) *J. Biochem. 89*, 337-339.
Kumar, V. V., Malewicz, B., & Baumann, W. J. (1989) *Biophys. J. 55*, 789-792.
Lichtenstein, A. H., Small, D. M., & Brecher, P. (1982) *Biochemistry 21*, 2233-2241.
Lowry, O. H., Rosebrough, N. J., Farr, A. L., & Randall, R. J. (1951) *J. Biol. Chem. 193*, 265-275.
Mabrey, S., & Sturtevant, J. M. (1977) *Biochim. Biophys. Acta 486*, 444-450.
Maggio, J. E. (1980) *Proc. Natl. Acad. Sci. U.S.A. 77*, 2582-2586.
Martin, M. L., Delpuech, J. J., & Martin, G. J. (1980) in *Practical NMR Spectroscopy*, Chapter 8, Heydem, London.
Mizuno, K., Toyosato, M., Tanimizu, I., & Hirakawa, H. (1980) *Anal. Biochem. 108*, 6.
Opella, S. J., Nelson, D. J., & Jardetzky, O. (1976) *J. Chem. Phys. 64*, 2533-2535.
Parks, J. S., Cistola, D. P., Small, D. M., & Hamilton, J. A. (1983) *J. Biol. Chem. 258*, 9262-9269.
Pauls, R. P., Mackey, A. L., & Bloom, M. (1983) *Biochemistry 22*, 6101-6109.
Powell, G. L., Tippett, P. S., Kiorpes, T. C., McMillan-Wood, J., Coll, K. E., Schulz, H., Tanaka, K., Kang, E. S., & Shrago, E. (1985) *Fed. Proc. 44*, 81-84.
Richards, E. W., Hamm, M. W., Fletcher, J. E., & Otto, D. A. (1990) *Biochim. Biophys. Acta 1044*, 361-367.
Schmidt, C. F., Barenholz, Y., Huang, C., & Thompson, T. E. (1978) *Biochemistry 16*, 3948-3954.
Shug, A. L., & Shrago, E. (1973) *J. Lab. Clin. Med. 81*, 214-218.
Smith, R. H., & Powell, G. L. (1986) *Arch. Biochem. Biophys. 244*, 357-360.
Spooner, P. J. R., Hamilton, J. A., Gantz, D. L., & Small, D. M. (1986) *Biochim. Biophys. Acta 860*, 345-353.
Sumper, M., & Trauble, H. (1973) *FEBS Lett. 30*, 29-34.
Tokayama, M., Itoh, S., Nagasaki, T., & Tanimizu, I. (1977) *Clin. Chim. Acta 79*, 93.
Wehrli, F. W., & Wirthlin, T. (1976) in *Interpretation of Carbon-13 NMR Spectra*, John Wiley & Sons, Chichester.
Whitmer, J. T., Idell-Wenger, J. A., Rovetto, M. J., & Neely, J. R. (1978) *J. Biol. Chem. 253*, 4305-4309.
Wolcowicz, P. E., Pownall, H. J., & McMillin-Wood, J. B. (1982) *Biochemistry 21*, 1990-1996.
Zahler, W. L., Barden, R. E., & Cleland, W. W. (1968) *Biochim. Biophys. Acta 164*, 1-11.

Rotational Motion of Monomeric and Dimeric Immunoglobulin E–Receptor Complexes†

Jeffrey N. Myers,‡ David Holowka, and Barbara Baird*
Department of Chemistry, Baker Laboratory, Cornell University, Ithaca, New York 14853-1301
Received May 9, 1991; Revised Manuscript Received September 5, 1991

ABSTRACT: Erythrosin 5′-thiosemicarbazide labeled immunoglobulin E (IgE) was used to monitor the rotational dynamics of monomeric and dimeric $Fc_\epsilon RI$ receptors for IgE on rat basophilic leukemia (RBL) cells using time-resolved phosphorescence anisotropy. Receptors were studied both on living RBL cells and on membrane vesicles derived from the RBL cell plasma membrane. The un-cross-linked IgE–receptor complexes on cells and vesicles exhibit rotational correlation times that are consistent with those expected for freely rotating monomers, but a small fraction of these complexes on cells may be rotationally immobile. A comparison of the initial phosphorescence anisotropy values for erythrosin-labeled IgE–receptor complexes on cells and vesicles reveals a fast component of rotational motion that is greater on the vesicles and may be due to a site of segmental flexibility in the receptor itself. Dimers of IgE–receptor complexes formed with anti-IgE monoclonal antibodies appear to be largely immobile on cells, but they are mobile on vesicles with a 2-fold larger rotational correlation time than the monomeric complexes. The results suggest that dimeric IgE–receptor complexes undergo interactions with other membrane components on intact cells that do not occur on the membrane vesicles. The possible significance of these interactions to receptor function is discussed.

Aggregation of $Fc_\epsilon RI$, the high-affinity receptor for immunoglobulin E (IgE)[1] on rat basophilic leukemia (RBL)[1] cells, results in cellular degranulation and the consequent release of histamine, as well as in the secretion of other inflammatory mediators during the allergic response [reviewed in Metzger et al. (1986), Siraganian (1988), and Beaven and Ludowyke (1989)]. The molecular mechanism by which aggregated receptors trigger a number of different signal transduction pathways that lead to these events remains largely unknown. Previous fluorescence photobleaching recovery measurements on RBL cells showed that most monomeric

† This work was supported by Grants AI18306 and AI22449 from the National Institutes of Health. J.N.M. was a predoctoral trainee of the National Institutes of Health (GM07273).
* Author to whom correspondence should be addressed.
‡ Present address: Department of Pathology, Columbia University College of Physicians and Surgeons, 630 W. 168th St., New York, NY 10032.

[1] Abbreviations: RBL, rat basophilic leukemia; IgE, immunoglobulin E; DNP, 2,4-dinitrophenyl; BSA, bovine serum albumin; IgE_m, mouse monoclonal anti-DNP IgE; IgE_r, rat myeloma IgE; IgE–R, IgE–receptor complex; Er, erythrosin 5′-thiosemicarbazide; HEPES, *N*-(2-hydroxyethyl)piperazine-*N*′-2-ethanesulfonic acid; HBS, HEPES-buffered saline.

0006-2960/92/0431-567$03.00/0

IgE–receptor complexes (IgE–R) are laterally mobile whereas aggregates of three and larger are immobile on the time scale of a photobleaching measurement (Menon et al., 1986a,b). These aggregates trigger substantial degranulation, whereas dimeric IgE–R are ineffective at triggering cellular degranulation in these cells (Fewtrell & Metzger, 1980) and show only a small reduction in lateral mobility (Menon et al., 1986a,b). In contrast to these results, dimeric complexes of $Fc_\epsilon RI$ made with some monoclonal antireceptor antibodies (in the absence of IgE) trigger substantial degranulation (Basciano et al., 1986; Ortega et al., 1988). The reason for these differences is presently unknown, but they suggest some control by IgE in the requirements for receptor activation.

The study of ligands that form small aggregates of IgE–R can be useful in distinguishing the essential from the incidental in the formation of an effective aggregate. Elucidation of the relationship between aggregation and function for this receptor has been hindered by a limited understanding of aggregate structure and dynamics. Rotational motion is sensitive to small changes in the aggregation state and local dynamics of membrane systems, and measurements of rotational mobility have been informative in many systems, including the receptor for IgE on RBL cells (Jovin & Vaz, 1989). Zidovetzki et al. (1986) measured the rotational dynamics of erythrosin isothiocyanate labeled IgE–R on living RBL cells using time-resolved phosphorescence anisotropy. They found that the monomeric IgE–R had a rotational mobility consistent with that expected for mobile receptors in a fluid cell membrane whereas extensive cross-linking with polyclonal anti–IgE immobilized IgE–R on the time scale of hundreds of microseconds.

In the present study, the rotational dynamics of monomeric and dimeric erythrosin-labeled IgE–R were investigated on living cells and on plasma membrane vesicles prepared from RBL cells. Receptors on these vesicles have lost much of the restriction on lateral mobility observed with intact cells (Holowka & Baird, 1983; Menon et al., 1986b), and they permit us to evaluate the complex interactions on living cells that might have physiological significance. Formation of IgE–R dimers was accomplished with two different monoclonal anti-IgE antibodies designated B1E3 and A2. B1E3 is a rat IgG that binds to a single site in the $C_\epsilon 4$ domains of mouse IgE (IgE_m; Keegan et al., 1991; Grassberger, 1989) and does not trigger cellular degranulation in the absence of additional cross-linking ligands (Posner, 1991). A2 binds to at least two sites in the Fc region of rat IgE (IgE_r), one of high affinity and one or more of low affinity (Conrad et al., 1983; Menon et al., 1986b). Stoichiometric concentrations of A2 with IgE produce IgE_r–R dimers, and higher concentrations of A2 produce larger aggregates of IgE_r–R. The degranulation response due to cross-linking with A2 is very poor in the dimer state but increases as the concentration is raised and larger complexes are formed (Menon et al., 1986b).

In this study, we find that the formation of dimeric IgE–R by both of these antibodies results in a large decrease in the extent of their phosphorescence anisotropy decay on cells, and this is inconsistent with the formation of mobile dimeric complexes which is observed with these antibodies on the membrane vesicles. The results suggest that formation of dimeric IgE–R causes them to interact with other cellular components in a manner that was not previously revealed by lateral diffusion measurements.

Experimental Procedures

Materials. Erythrosin 5′-thiosemicarbazide (Er) was custom-synthesized by Molecular Probes Inc. and was used without further purification. ^{3}H-5HT was from Dupont NEN. Glucose oxidase (≈180 000 Sigma units/mg of solid; 98% of activity due to glucose oxidase) was from Sigma Chemical Co., and argon was prepurified grade (O_2 < 5 ppm). The murine monoclonal anti-2,4-dinitrophenyl (DNP) IgE (IgE_m; Liu et al., 1980) and polyclonal rabbit anti-IgE_m and anti-IgE_r were purified as previously described (Holowka & Metzger, 1982). IgE_m was labeled with ^{125}I using chloramine T (Holowka & Baird, 1983a). Purified rat myeloma IR162 IgE (IgE_r) was a gift from Dr. John Hakimi at Hoffmann–La Roche (Nutley, NJ). The multivalent ligand DNP_{27}-BSA (DNP-BSA) was prepared as previously described (Eisen et al., 1959) and exhibited a single major band at M_r ~68 000 on an SDS–polyacrylamide gel. The mouse anti-IgE_r hybridoma cell line A2 (Conrad et al., 1983) was obtained from Dr. Daniel Conrad (Virginia College of Medicine, Richmond, VA) and grown in mice; the antibody was purified from the ascites fluid by ammonium sulfate precipitation followed by anion-exchange chromatography on a Pharmacia Mono Q column. The purified monoclonal rat anti-IgE_m antibody B1E3 was a gift from Dr. Conrad. $F(ab)'_2$ fragments of A2 were prepared by digestion with pepsin as previously described (Holowka et al., 1985). This preparation showed a major band on an unreduced SDS–polyacrylamide gel that migrated with a $M_r \simeq$ 100K, as well as a small amount of undigested antibody at $M_r \simeq$ 150K that appeared to represent <10% of the total protein.

RBL Cells and Plasma Membrane Vesicles. RBL cells, subline 2H3 (Barsumian et al., 1981), were maintained in stationary culture as described (Taurog et al., 1979). The cells were harvested with 1.5 mM EDTA in a saline/HEPES buffer, centrifuged at 200*g*, and then resuspended to a density of 10^7/mL in 135 mM NaCl, 5 mM KCl, 1.8 mM $CaCl_2$, 1 mM $MgCl_2$, 5.6 mM glucose, and 20 mM HEPES, pH 7.4 (HBS), with 0.1% BSA (HBS–BSA). RBL cell plasma membrane vesicles were prepared as described previously (Baird & Holowka, 1985) and dialyzed into 135 mM NaCl, 5 mM KCl, 20 mM HEPES, and 0.01% NaN_3, pH 7.4. These vesicles are mostly right-side-out, large (0.1–10-μm diameter), unilamellar, and free of cytoplasmic organelles and a cytoskeletal network (Holowka & Baird, 1983a).

Preparation, Purification, and Testing of Er–IgE. Purified IgE_r and IgE_m were derivatized with Er following mild oxidation of terminal sugars (Lotan et al., 1975) as follows. Between 0.5 and 1.0 mg of IgE at a concentration of about 5 μM was dialyzed into a sulfate buffer (0.1 M sodium sulfate, 1 mM EDTA, and 20 mM sodium phosphate, pH 5.7), then sodium periodate was added to the IgE solution at a final concentration of 5 mM, and the mixture was incubated for 20 min at room temperature. The periodate was removed from the reaction mixture by centrifugation for 2 min at 850*g* through a 1 × 5 cm column of Sephadex G-50 Fine (Pharmacia) equilibrated with pH 7.0 sulfate buffer. All subsequent manipulations were carried out in dim light to minimize photodecomposition. Er was added at a 5-fold molar excess over IgE from a solution of 10 mM Er in DMSO and allowed to react for 1 h at room temperature. The reaction mixture was then centrifuged at 10000*g* for 3 min to remove small amounts of insoluble material. Free Er was removed by centrifugation over a Sephadex column as above, and the mixture was dialyzed exhaustively against pH 7.0 sulfate buffer.

In some preparations of Er–IgE_m, a trace amount of ^{125}I-IgE_m was added to the reaction mixture to monitor the IgE concentration. The concentration of IgE_m before the reactions

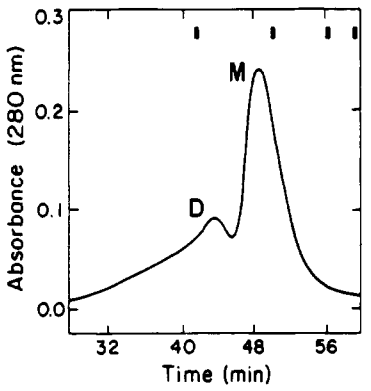

FIGURE 1: Gel permeation chromatographic analysis of IgE_m modified with erythrosin thiosemicarbazide as described in the text. Molecular weight standards are indicated with bars; from left to right, 670K, 158K, 44K, and 17K. The peaks corresponding to monomeric and dimeric IgE derivatives are indicated by M and D, respectively. The void volume of the column is at 24-min elution time.

was determined from absorbance measurements (ϵ_{280} = 3.0 × 10^5 M^{-1} cm^{-1}; Liu et al., 1980), and the specific activity (cpm per microgram) was calculated as described (Holowka & Baird, 1983a). To calculate the concentrations of Er and IgE in the conjugates, the absorbance of Er at 536 nm (ϵ = 83 000 M^{-1} cm^{-1}; Moore et al., 1979) was used to correct for the contribution of Er to the 280-nm absorbance (ϵ_{280nm} = 32 000 M^{-1} cm^{-1}). The IgE concentration calculated from the corrected value agreed with the IgE concentration determined from the radioactive tracer. The molar ratio of Er to IgE was 2.7:1 and 3.7:1 in two different preparations following exhaustive dialysis. Under these conditions, 1.0 Er per IgE was obtained in the absence of oxidation by sodium periodate.

Gel permeation chromatography was performed with Er–IgE using a Superose 6 column (Pharmacia) connected to a Waters HPLC system equipped with a 280-nm detector. Molecular weight standards (Bio-Rad) and unlabeled IgE were run under the same conditions to provide calibration. In addition to the monomeric Er–IgE peak, a significant amount of higher molecular weight material was observed, corresponding to oligomers of Er–IgE (Figure 1). In some samples, a small late peak corresponding to free Er was also present (not shown). Fractions were collected corresponding to monomeric and dimeric IgE as determined using the molecular weight standards. After chromatography, the ratio of Er to IgE was reassessed and was found to be approximately 1:1 for the monomer fractions. The oligomeric fractions were more heavily modified with Er; the dimer fraction contained about 3.6 Er per IgE.

The binding of the Er–IgE_m to RBL cells was assessed with the ^{125}I-labeled Er–IgE (Kulczycki & Metzger, 1974). Nonspecific binding was assessed by addition of labeled Er–IgE after blocking the IgE–receptors with a 20-fold excess of unlabeled IgE, and was less than 7% of the total bound IgE. The amount of IgE specifically bound per cell agreed with the typical number of receptors per cell, between 200 000 and 300 000 (Barsumian et al., 1981). HPLC-purified monomeric Er–IgE fractions were added to cells either with or without the multivalent ligand DNP_{27}-BSA or polyclonal anti-IgE, and the ^{3}H-5HT release was compared to that of cells to which unmodified IgE had been added (Baird et al., 1983). With the monomeric Er–IgE, the release of ^{3}H-5HT was negligible in the absence of the cross-linkers; in the presence of the cross-linkers DNP_{27}-BSA or polyclonal anti-IgE, release of ^{3}H-5HT was comparable to that observed with unmodified IgE (typically ~50–70% of the total at optimal concentrations of antigen; data not shown).

Preparation of Samples for Phosphorescence Measurements. RBL cells in HBS–BSA at a concentration of 10^7/mL were split into two equal portions. One portion ("sample") was labeled with Er–IgE at 10 μg/mL, and the other portion ("blank") was maintained in parallel throughout all of the manipulations, but without addition of Er–IgE. The suspensions were incubated at 37 °C for 1.5 h to allow the Er–IgE to bind to $Fc_\epsilon RI$ and then washed twice with HBS. Both samples were resuspended in HBS to a concentration of 10^7/mL, and kept suspended by gentle rotation at 4 °C until use. Measurements were performed with the cells at either 10^7/mL or 5 × 10^6/mL, and unless otherwise specified, all of the experiments were carried out at 25 °C. The samples were deoxygenated by a combination of a glucose oxidase enzyme system (Englander et al., 1987) and gentle flow of humidified argon over the suspension. The viability of the cells was checked by Trypan Blue exclusion and was 90–95% both before and after the anisotropy measurement.

Membrane vesicles were labeled with a 3–5-fold excess of Er–IgE over receptors as previously described for fluorescent derivatives of IgE (Holowka & Baird, 1983b). Under these conditions, >90% of the Er–IgE binding is blocked by excess unlabeled IgE, and membrane samples in which specifically bound Er–IgE is absent give virtually no background signal under the conditions of the phosphorescence anisotropy experiments. For both cells and membrane vesicles, there are no detectable changes in the anisotropy decay curves for Er–IgE-labeled samples incubated at 4 °C over the course of several hours or at 25 °C for 60 min, indicating that Er–IgE dissociation from receptors or other changes are not significant during the time of data collection. This is consistent with the previously characterized slow rate of dissociation of IgE from $Fc_\epsilon RI$ (Kulczycki et al., 1974; Metzger et al., 1986).

Time-Resolved Phosphorescence Anisotropy Measurements. Phosphorescence emission was induced with 532-nm excitation light from a frequency-doubled Nd:YAG laser (Quanta-Ray DCR-1), that was polarized with a Glan–Thompson prism. The stirred, thermostated sample chamber held a 1 cm × 1 cm path length fused silica cuvette for measurements on cells, and 5 mm × 5 mm path length fused silica cells for the vesicle measurements. T-Format collection was used, with emission above 650 nm selected by a Schott KV-550 filter followed by a Schott RG-645; 45-mm-diameter sheet polarizers (Melles–Griot) in rotating mounts separated the polarized emission components. Commercially gated photomultipliers (Thorn-EMI 9816) were used for detection, and the amplified signals for each channel were digitized at 3.125 MHz with a two-channel 25-MHz 8-bit A/D board (Sonotek STR-8000) in an IBM-AT computer. Signal-averaging was accomplished with software (Myers, 1990). The cumulative laser power was measured and recorded for each averaged decay to correct for any long-term drift in the laser output. Usually 10 000 decays were recorded at a rate of 10 Hz, resulting in an acquisition time of about 17 min. Two additional sets of decays were acquired during each experiment to determine the *g* factor (see below). At least 10 min (usually 17 min) was allowed to elapse after addition of a ligand to the cell sample and before data acquisition. This allowed time for binding of the ligands and removal of oxygen from the added ligand-containing solution (usually <3% of the total sample volume). The total amount of time that a typical sample would be exposed to the ligand by the end of the measurement was about 35 min.

Data Analysis. After correction for any changes in laser input power during the experiment, the blank decays (unlabeled cells) were subtracted from the sample decays, to correct

for the autoluminescence background of the cells. The calculation of resultant difference, total intensity, and anisotropy curves followed the formalism given in Jovin and Vaz (1989), in which the total intensity decay is corrected for the effects of the finite aperture of the emission optics (h) and detector sensitivity to polarized light (g). The difference between the two orthogonal emission channels, $d(t)$, is thus given by $d(t) = I_{\parallel}(t) - gI_{\perp}(t)$, the total intensity decay, $S(t)$, of the erythrosin is given by $S(t) = I_{\parallel}(t) + ghI_{\perp}(t)$, and the anisotropy, $r(t)$, is given by $r(t) = d(t)/S(t)$. $I_{\parallel}(t)$ and $I_{\perp}(t)$ are the emission components parallel and perpendicular to the excitation polarization, respectively, g accounts for the difference in detector sensitivity for $I_{\parallel}$ and $I_{\perp}$, and is determined as the ratio of the parallel to the perpendicular emission intensities when the excitation polarizer is in the perpendicular position. The aperture correction, h, has a value of 1.75 in our system (Myers, 1990); for small-aperature light collection systems, h approaches 2 (Jovin & Vaz, 1989). Three exponentials were required to fit the total intensity decay curves, and the anisotropy decays were adequately fit to a single exponential plus a residual anisotropy using a weighted nonlinear least-squares fitting routine:

$$r(t) = (r_0 - r_\infty)e^{-t/\phi} + r_\infty \quad (1)$$

where r_0 is the initial anisotropy, r_∞ is the residual anisotropy, and ϕ is the rotational correlation time. Calculation of variances for $I_{\parallel}(t)$ and $I_{\perp}(t)$ and propagation of error for the fitting procedure are described in Myers (1990).

Results

Monomeric IgE–Receptors Complexes. Before investigation of the behavior of IgE–R aggregates, measurements were first performed on monomeric IgE–R on living RBL cells and on vesicles derived from RBL cell plasma membranes. IgE_r and IgE_m were modified with Er, which reacts with oxidized terminal sugars in the glycosylation sites on the Fc and Fab regions of IgE (Ishida et al., 1982) to form a stable thiosemicarbazone (Cherry et al., 1980). Phosphorescence emission from dyes like Er arises from an excited triple state, and the observed emission usually contains multiple components (Zidovetzki et al., 1986). In our experiments at 25 °C, the intensity decay was resolved into three components, with normalized amplitudes and lifetimes of 0.26 and 13 μs, 0.35 and 46 μs, and 0.39 and 180 μs, respectively. In all of the experiments described here, the phosphorescence decay was unchanged by cross-linking the IgE–R and was similar on cells and vesicles. In temperature dependence studies, both the lifetimes and the phosphorescence intensity decreased with increasing temperature, as expected.

The time-resolved phosphorescence anisotropy of Er–IgE_r bound to receptors on cells at 25 °C is shown in Figure 2, sample a. As in all of the experiments described here, the anisotropy decays can be fit by a single rotational correlation time, ϕ (eq 1), and this is shown as the smooth continuous line through the data points. The initial anisotropy (r_0) is positive and decays to a lower, positive residual value (r_∞), and this is consistent with the modification of IgE at several randomly oriented sites (see Discussion). As summarized in Table I, the values of ϕ for cell-bound Er–IgE–R range from 19 μs at 36 °C to 68 μs at 12 °C and agree with previously published results obtained with erythrosin isothiocyanate labeled IgE_r on RBL cells (Zidovetzki et al., 1986). It is noteworthy that the values for r_0 and the residual anisotropy r_∞ also decrease with increasing temperature. These changes are in accord with the increases in fast probe and protein segmental motions

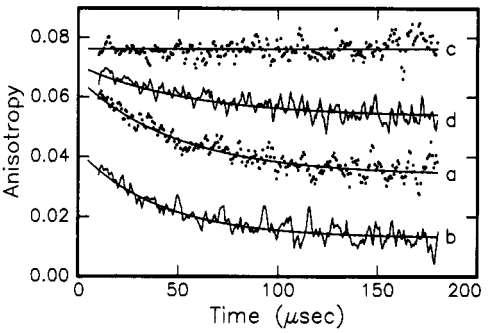

FIGURE 2: Anisotropy decay of monomeric IgE–R on RBL cells and vesicles. Representative anisotropy decays for monomeric IgE_r–R on cells (a) and membrane vesicles (b) at 25 °C are shown as described in the text. Sample c shows the anisotropy decay for IgE_r–R on cells after cross-linking the IgE–R with anti-IgE_r at 4.5 μg/mL. Sample d shows the anisotropy decay for IgE_r–R on vesicles after cross-linking with anti-IgE_r at 2.2 μg/mL. The smooth lines through the data represent fits to eq 1. For curve a, $r_0 = 0.066$, $r_\infty = 0.034$, and $\phi = 50$ μs; for curve b, $r_0 = 0.042$, $r_\infty = 0.013$, and $\phi = 41$ μs; for curve c, $r_0 = r_\infty = 0.076$, and for curve d, $r_0 = 0.071$, $r_\infty = 0.053$, and $\phi = 61$ μs.

Table I: Temperature Dependence of the Anisotropy Decay of Monomeric IgE–R[a]

T (°C)	r_0	r_∞	r_∞/r_0[b]	ϕ (μs)
12	0.086 (0.001)	0.053 (0.001)	0.62 (0.02)	68 (6)
19	0.080 (0.001)	0.048 (0.001)	0.59 (0.01)	39 (3)
27	0.078 (0.002)	0.043 (0.001)	0.55 (0.01)	23 (2)
36	0.066 (0.004)	0.036 (0.004)	0.55 (0.03)	19 (2)

[a] The data shown are from one experiment at each temperature, performed on the same day with the same cells and Er–IgE_m (preparation 2). The uncertainties listed in parentheses are the standard deviations from weighted nonlinear least-squares fits of the anisotropy decay curves to eq 1. [b] The uncertainties for the ratios of r_∞/r_0 were propagated from the standard deviations of the data from the fits, as listed for r_0 and r_∞.

expected with increasing temperature. The ratio of r_∞/r_0 decreases only slightly with increasing temperature, from 0.62 at 12 °C to 0.55 at 36 °C (Table I). Thus, the r_∞/r_0 parameter does not appear to be very sensitive to changes in the submicrosecond motions that change r_0, consistent with a random orientation of the Er emission dipoles (see Discussion).

The results for monomeric Er–IgE preparations bound to RBL cell plasma membrane vesicles differ in several respects from those on the cells. A typical anisotropy decay for monomeric IgE_r–R on vesicles at 25 °C is shown in Figure 2, sample b. The initial anisotropy for vesicle-bound Er–IgE–R is consistently lower than that for the corresponding cell-bound Er–IgE–R, and this is seen for both IgE_r and IgE_m (Table II). This indicates that there is at least one component to the anisotropy decay with a correlation time on the submicrosecond time scale that contributes to the value of r_0 to a greater extent in the vesicle samples than in the cell samples. For reasons discussed below, it seems likely that this component is due to segmental flexibility in the receptor itself that is greater in the vesicle sample (see Discussion). The time courses of the anisotropy decays are similar in cell and vesicle samples, and Table II shows that the values of ϕ for monomeric IgE–R on cells and vesicles are very similar for both IgE_r and IgE_m. In contrast, not only r_0 but also r_∞ and r_∞/r_0 are significantly lower for these monomeric complexes on vesicles than on cells. It is notable that r_∞/r_0 is ~40% smaller on vesicles than on cells, and this difference is the same for both IgE_r and IgE_m, even though they have significantly different values for r_0. It is thus unlikely that the differences in r_∞/r_0 are merely a result of the lower r_0 values on vesicles, but rather it appears that

Table II: Anisotropy Decay Parameters for Monomeric IgE–R on RBL Cells and RBL Cell Plasma Membrane Vesicles[a]

sample	r_0	r_∞	r_∞/r_0	ϕ (μs)
IgE_r				
(1) vesicles (n = 2)	0.042 (0.001)	0.014 (0.001)	0.33 (0.03)	44 (4)
(2) cells (n = 6)	0.059 (0.010)	0.032 (0.005)	0.53 (0.02)	47 (16)
IgE_m				
(3) vesicles (n = 4) (prepn 2[b])	0.060 (0.002)	0.023 (0.003)	0.40 (0.05)	40 (7)
(4) cells (n = 4) (prepn 1)	0.066 (0.002)	0.037 (0.004)	0.57 (0.04)	49 (14)
(5) cells (n = 3) (prepn 2)	0.073 (0.006)	0.045 (0.006)	0.62 (0.08)	42 (21)

[a] All experiments were performed at 25 °C. Averages were calculated from the results of individual experiments. Uncertainties in parentheses represent the standard deviations of the data used to calculate the averages (n = number of experiments). The parameters for individual data sets used in the calculation of the averages were in all cases derived from weighted fits of the data to eq 1. [b] Prepn 1 and prepn 2 refer to two different preparations of Er–IgE_m used in these experiments.

Table III: Anisotropy Decay Parameters for Aggregated IgE–R on RBL Cells and Vesicles[a]

sample	r_0	r_∞	r_∞/r_0	ϕ (μs)
		IgE_r Vesicles[b]		
A2 F(ab)′$_2$				
(1) 15 nM	0.059	0.023	0.39	102
A2 intact				
(2) 15 nM	0.064	0.032	0.50	81
(3) 150 nM	0.066	0.042	0.63	110
anti-IgE_r (n = 2)				
(4) 2.2 μg/mL	0.071 (0.001)	0.050 (0.004)	0.71 (0.04)	79 (25)
		IgE_r Cells		
A2 F(ab)′$_2$ (n = 2)				
(5) 7–12 nM	0.064 (0.008)	0.052 (0.008)	0.82 (0.01)	24 (10)
A2 intact (n = 2)				
(6) 7–10 nM	0.072 (0.002)	0.059 (0.003)	0.82 (0.02)	69 (42)
(7) 70–100 nM	0.073 (0.001)	0.066 (0.001)	0.90 (0.01)	59 (43)
anti-IgE_r (n = 2)				
(8) 4 μg/mL	0.075 (0.002)	0.075 (0.002)	1.00 (0.03)	ND[c]
		IgE_m Vesicles		
B1E3 (n = 2)				
(9) 22 nM	0.081 (0.004)	0.031 (0.008)	0.38 (0.12)	74 (8)
(10) 110 nM	0.085 (0.006)	0.037 (0.003)	0.44 (0.06)	60 (2)
DNP_{27}-BSA				
(11) 4 μg/mL	0.094 (0.001)	0.069 (0.002)	0.74 (0.02)	67 (13)
anti-IgE_m				
(12) 4 μg/mL	0.099 (0.011)	0.081 (0.001)	0.82 (0.01)	48 (11)
		IgE_m Cells		
B1E3 (n = 3)				
(13) 80–110 nM	0.079 (0.005)	0.066 (0.003)	0.83 (0.02)	122 (148)
DNP_{22}-BSA (n = 2)				
(14) 4 μg/mL	0.077 (0.002)	0.075 (0.002)	0.97 (0.04)	ND
anti-IgE_m (n = 2)				
(15) 4 μg/mL	0.086 (0.002)	0.086 (0.002)	1.00 (0.03)	ND

[a] All experiments were performed at 25 °C. The numbers in parentheses represent averages of the standard deviations of the individual data sets. [b] For IgE_r vesicles, the results are shown for individual experiments with each cross-linker. [c] ND = not determined because change from r_0 to r_∞ was not significant compared to the level of noise.

they may reflect an immobile fraction on the cells (see Discussion).

Overall, the quality of the data with vesicles is higher than that for the cells, despite the lower initial anisotropy values. This is primarily because the background emission from the vesicles is negligible after only a few microseconds while the background emission from cells is significant for tens of microseconds (data not shown). Tumbling of the vesicles does not contribute significantly to the decay characteristics, as the anisotropy decays level off after about 200 μs, as seen in Figure 3.

Figure 2, sample c, shows a representative anisotropy decay after extensive cross-linking of IgE_r–R with polyclonal anti-IgE_r on cells. As expected from Zidovetzki et al. (1986), immobilization of IgE_r–R occurs under these conditions, such that no significant change in the anisotropy is apparent over the time course of the experiment. Also, r_0 is higher for the aggregates than for monomeric IgE–R. Under the conditions of our experiments, little internalization of IgE–R is expected to occur during the time of measurements (Robertson et al., 1986). As seen in Figure 2, sample d, cross-linking of IgE–R by anti-IgE on membrane vesicles results in a large reduction in the phosphorescence anisotropy decay compared with monomeric IgE–R on vesicles (curve b). This is also indicated by the relatively large values for r_∞/r_0 for this case, as well as for IgE–R aggregated by the multivalent antigen DNP_{27}-BSA on both cells and vesicles (Table III). For both of these cross-linking agents, the loss of phosphorescence anisotropy decay is usually greater on cells than on membrane vesicles. The similar values of r_0 for extensively cross-linked Er–IgE–R on cells and vesicles (Figure 2 and Table III) indicate that the differences in r_0 seen with monomeric Er–IgE–R for cells and vesicles are not due to an artifact of light scattering or background subtraction.

Rotational Mobility of IgE–R Dimers. The anisotropy decay of IgE_r–R cross-linked with stoichiometric concentrations of A2 F(ab)′$_2$ to produce IgE–R dimers on vesicles at 25 °C is shown in Figure 3, sample b. Anisotropy parameters

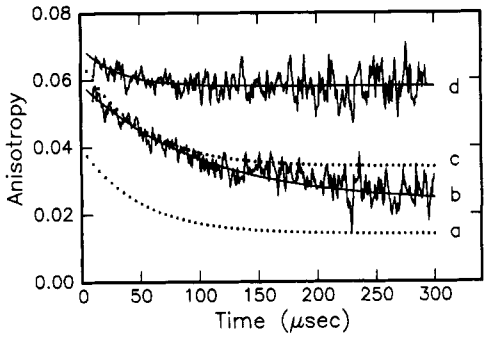

FIGURE 3: Anisotropy decays of IgE_r–R cross-linked with A2 on RBL cells and vesicles. The dotted curve (a) shows the single-exponential fit to the anisotropy decay data for monomeric IgE_r–R on vesicles, with $r_0 = 0.040$, $r_\infty - 0.014$, and $\phi = 49$ μs. The data in (b) represent the anisotropy decay on vesicles after cross-linking the IgE–R with 15 nM $F(ab)'_2$ of A2, and the smooth line through the data shows the best fit with parameters $r_0 = 0.059$, $r_\infty = 0.023$, and $\phi = 102$ μs. The dotted curve (c) shows the single-exponential fit to the anisotropy decay data for monomeric IgE–R on cells, with $r_0 = 0.066$, $r_\infty = 0.034$, and $\phi = 50$ μs. The data in (d) represent the anisotropy decay on cells after cross-linking the IgE–R with 7.4 nM $F(ab)'_2$ of A2, and the smooth line through the data shows the best fit with $r_0 = 0.070$, $r_\infty = 0.058$, and $\phi = 31$ μs. All data were taken at 25 °C.

for these data are included in Table III. The fit to eq 1 for monomeric IgE–R before addition of A2 in this experiment is shown in Figure 3, sample a, and included in Table II. The rotational mobility of the A2-cross-linked IgE–R dimers on vesicles appears to be reduced compared to monomers, such that the value of ϕ is about twice that of the monomeric complexes. The value for r_0 also increases, but r_∞/r_0 is little changed for the dimers (compare Table III, line 1, with Table II, line 1). $F(ab)'_2$ fragments were used to prevent potential interactions of the Fc regions of the bound A2 antibodies with Fcγ receptors (Segal et al., 1981), but qualitatively similar anisotropy decays were obtained when these experiments were carried out with whole A2 at the same concentrations (Table III, line 2). At higher concentrations of A2 that cause of the formation of longer chains of IgE–R (Menon et al., 1986b), the value of ϕ for the mobile IgE–R is similar to that for dimer-forming concentrations of A2, but the value of r_∞/r_0 is in between that for dimers and large aggregates made with polyclonal anti-IgE (Table III, lines 3 and 4).

The anisotropy decay for A2 $F(ab)'_2$-cross-linked IgE–R dimers on cells is shown in Figure 3, sample d (parameters for fit included in Table III), and sample c shows a smooth curve corresponding to the fit to the data for monomeric IgE–R on cells before addition of A2 (parameters included in Table III). It is apparent that little anisotropy decay occurs for A2 dimers on cells ($r_0 \simeq r_\infty$) and this is reflected in the high value of r_∞/r_0 (Table III, line 5). As with vesicles, whole A2 on cells causes similar results as its $F(ab)'_2$ fragment; that is, most of the dimeric IgE–R on cells were found to be immobile on the time scale of the measurement ($r_0 \simeq r_\infty$; Table III, line 6). Higher concentrations of A2 also yielded similar results (Table III, line 7). In these cases, the small amount of residual decay of anisotropy has values for ϕ that are less than 100 μs, and this may be due to a small fraction of uncross-linked or dimeric IgE–R.

Anisotropy decay of vesicle-bound IgE_m–R cross-linked by the monoclonal anti-IgE_m B1E3 is shown in Figure 4A, and the decay parameters for several experiments are included in Table III. The results with B1E3 at 22 nM (Sample b) and 110 nM (sample c) are nearly identical, with the higher concentration yielding only slightly higher values of r_0 and r_∞. The values of ϕ are similar at both low and high concentrations, and are 1.5–2.0 times longer than ϕ for monomeric

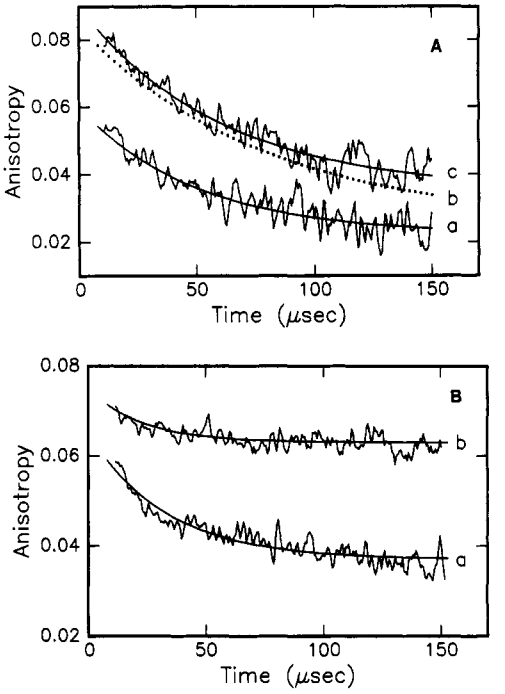

FIGURE 4: Anisotropy decays of IgE–R cross-linked with B1E3 on RBL membrane vesicles (A) and on cells (B). (A) The anisotropy decays of IgE–R cross-linked with 22 (b) or 110 nM (c) B1E3 are compared to the decay of monomeric IgE–R (a). The smooth curves represent fits of the data of eq 1; for clarity, only the fit (dotted line) is plotted for 22 nM B1E3. B1E3 was added to a single sample to prepare samples a, b, and c in succession. The decay parameters for monomeric IgE–R are $r_0 = 0.060$, $r_\infty = 0.022$, and $\phi = 50$ μs. For the B1E3-cross-linked samples, the parameters at 22 nM B1E3 are $r_0 = 0.084$, $r_\infty = 0.025$, and $\phi = 79$ μs, and at 110 nM B1E3, $r_0 = 0.090$, $r_\infty = 0.035$, and $\phi = 60$ μs. (B) The anisotropy decay for IgE–R cross-linked with 106 nM B1E3 (b) on RBL cells is shown together with the decay for monomeric IgE–R (a), and the smooth curves are the fits of the data to eq 1. The decay parameters for (a) are $r_0 = 0.065$, $r_\infty = 0.037$, and $\phi = 33$ μs; for (b), the fitted parameters are $r_0 = 0.075$, $r_\infty = 0.063$, and $\phi = 23$ μs.

IgE–R (sample a). This is consistent with the formation of dimers of IgE–R via a single binding site for B1E3 on IgE_m which is nearly saturated at both the concentrations used (Grassberger, 1989).

As seen in Figure 4B, B1E3 cross-linking of IgE–R on cells produces substantial increases in r_0, and there is little decay in the anisotropy on the time scale of the experiment ($r_0 \simeq r_\infty$). Additional cross-linking with either polyclonal anti-IgE_m or DNP_{27}-BSA on cells causes little further change in the anisotropy decays caused by B1E3 alone (Table III). Thus, the principal observation from these experiments is that dimer-level cross-linking of IgE–R induces a much greater decrease in phosphorescence anisotropy decay on the cells than on vesicles.

Discussion

The present study extends the previous observations of Zidovetzki et al. (1986) on the rotational dynamics of IgE–R. Our experiments employed IgE that is labeled with a thiosemicarbazide derivative of erythrosin, following oxidation of the terminal sugars of the carbohydrate moieties to aldehydes (Cherry et al., 1980). Potential glycosylation sites are present in all four constant domains of rodent IgE (Ishida et al., 1982), so it is likely that there is a distribution of Er covalently attached in both the Fab and Fc segments. The modification appears to cause some limited aggregation of the IgE, and the aggregates have a higher average stoichiometry of labeling

than monomeric Er–IgE. When these aggregates were examined after separation by gel permeation chromatography (Figure 1), they were found not to bind detectably to RBL cells or to stimulate cellular degranulation (data not shown). The monomeric Er–IgE–R derivatives of both IgE_r and IgE_m have phosphorescence emission intensities similar to the erythrosin 5′-isothiocyanate derivative of IgE that was previously employed (data not shown; Zidovetzki et al., 1986). However, we find that the r_0 values for Er–IgE–R are somewhat greater than those of the isothiocyanate derivatives (J. N. Myers, unpublished observations), and this results in smaller uncertainties in the anisotropy decay curves because of greater differences between the polarized emission components.

Despite these differences in the nature of the erythrosin modification of IgE and the corresponding r_0 values, our single-exponential values for ϕ of monomeric IgE–Rb on both cells and membrane vesicles are very similar to those obtained by Zidovetzki et al. (1986). Two components of diffusion are expected for simple uniaxial rotation (Rigler & Ehrenberg, 1973), but the quality of the data that can be obtained with nanomolar concentrations of labeled receptors as in the present case does not warrant a more precise interpretation in terms of rotational diffusion coefficients. The ranges of values for ϕ determined for monomeric IgE–R (Tables I and II) are similar to those reported for other membrane proteins with multiple membrane-spanning segments (Jovin & Vaz, 1989). However, as recently discussed by Rahman et al.,[2] these values are larger than expected for an IgE–R with seven predicted membrane-spanning regions (Blank et al., 1989) that is undergoing axial rotation perpendicular to the plane of a fluid membrane bilayer. The reason for this is not clear, and further experiments are needed to investigate this issue.

The mobility of dimers on vesicles, with ϕ values that are about 2-fold greater than those for monomers (Table III), is consistent with a simple fluid membrane environment in which dimer formation effectively doubles the intramembranous receptor volume (Saffman & Delbruck, 1975). This was seen with two different monoclonal anti-IgE antibodies that bind to the Fc region of IgE (A2 and B1E3, Table III and Figures 3 and 4), and we have also observed this with a bivalent hapten that cross-links via IgE antibody combining sites and efficiently forms cyclic dimers (Posner, 1991; Myers, 1990). The loss of anisotropy decay of these same dimeric IgE–R on intact cells (Figures 3 and 4 and Table III, and data not shown) suggests that interactions occur between these dimeric receptor aggregates and other components of the intact cells that are not maintained with the membrane vesicles (see below).

Whereas the ϕ values reflect the motions of IgE–R occurring on a microsecond time scale, the r_0 values reflect faster processes, such as local probe reorientation and internal protein motions. These motions occurring on the submicrosecond time scale reduce r_0 from its spectroscopically limiting value (0.25–0.28 for Er; Garland & Moore, 1979) and could include segmental motions of IgE and/or its receptor. The consistently smaller values of r_0 for monomeric Er–IgE–R on membrane vesicles compared with those on cells (Figure 2 and Table II) are not likely to be due to different amounts of local probe reorientation, because the values of r_0 for extensively cross-linked Er–IgE–R are similar for vesicles and for cells (Table III). Under these latter conditions, it is likely that local probe reorientation is the major determinant of r_0. Segmental motion within receptor-bound IgE is very limited on membrane vesicles and becomes negligible in the presence of a bivalent ligand (Holowka et al., 1990; Y. Zheng, D. Holowka, and B. Baird, unpublished observations). This segmental motion could contribute to the value of r_0 for un-cross-linked IgE–R on both cells and vesicles. We think it is unlikely that this limited segmental motion within IgE is signficantly greater on membrane vesicles than on cells. It is more likely that there is a site in the receptor itself that shows more flexibility on membrane vesicles than on cells. Previous nanosecond fluorescence depolarization studies with dansyllysine in the combining sites of anti-dansyl IgE revealed a mode of motion for membrane-bound IgE–R with a rotational correlation time of several hundred nanoseconds that may reflect this receptor segmental motion (Holowka et al., 1990). The apparent lower density of membrane proteins in the vesicles (Erickson et al., 1991; J. Erickson, unpublished observations) as well as the likelihood of some differences in the local lipid and/or protein environment of receptors on cells and vesicles makes it reasonable that there could be a greater amount of the segmental motion of the IgE binding domain of the receptor on vesicles compared with that on cells. Future studies using fluorescence depolarization with labeled anti-receptor Fab fragments will be carried out to evaluate this possibility directly.

In addition to the difference in r_0 for monomeric IgE–R on cells and vesicles, there is a significantly greater value of r_∞/r_0 for IgE–R on cells compared with that for vesicles, and this suggests the possibility of a rotationally immobile population of receptors on cells. Whereas r_0 reflects all motions occurring before observation of the phosphorescence decay, r_∞ reflects the equilibrium distribution of the probe and includes all motions, both fast and slow. Differences in r_∞ usually reflect differences in the fraction of species that are capable of undergoing rotation. To calculate the immobile fraction (f_{im}) of labeled species, r_∞ can be normalized to r_0, and theoretical and experimental values compared (Kawato & Kinosita, 1981):

$$f_{im} = \frac{(r_\infty/r_0)_{ex} - (r_\infty/r_0)_{th}}{1 - (r_\infty/r_0)_{th}} \quad (2)$$

The subscript "th" donotes the theroretical expectation value for r_∞/r_0 for 100% rotational mobility, and "ex" denotes the experimentally observed value of r_∞/r_0. If we assume that 100% of the IgE–R in the vesicle membranes are mobile, the r_∞/r_0 values in Table II for vesicles can be used as the theoretical $(r_\infty/r_0)_{th}$ values in eq 2. The r_∞/r_0 values in Table II for cells are then used as $(r_\infty/r_0)_{ex}$ in eq 2, yielding immobile fractions of 30% (±6%) for IgE_r and 36% (±16%) for IgE_m. Despite the large uncertainties involved in these estimates, it is reasonable to conclude that a small fraction of the IgE–R may be rotationally immobile in RBL cells.

These estimates must be interpreted cautiously. The immobile fraction calculated in eq 2 is very sensitive to small changes in the parameters used. For example, a lower limit estimate of 0.50 for $(r_\infty/r_0)_{ex}$ would yield values for f_{im} of 17–25%. It is also possible that the differences in r_∞/r_0 for cells vs vesicles could reflect differences in the extent of orientation of the emission dipoles for these two cases. As described by Kinosita et al. (1984), the value of r_∞/r_0 is expected to be greater for less flexible molecules with a smaller average cone angle for the distribution of emission dipoles about the principal axis of rotation. Alternatively, the immobile fraction estimated after a few hundred microseconds may simply be mobile on a much slower time scale, as suggested be recent studies on the acetylcholine receptor (Velez et al., 1990). It is notable that the estimated ≈20–30% rotationally immobile

[2] N. A. Rahman, I. Pecht, D. A. Roess, and B. G. Barisas, submitted for publication.

IgE–R on cells in the absence of cross-linking is similar to that for laterally immobile monomeric IgE–R as measured by fluorescence photobleaching recovery (Menon et al., 1986). Simultaneous lateral and rotational immobilization was observed previously for band 3 in erythrocytes (Tsuji et al., 1988), where it was attributed to interactions with the membrane cytoskeleton. The functional significance of a subpopulation of immobile, monomeric IgE receptors remains to be determined.

The dramatic loss of phosphorescence anisotropy decay seen with dimeric IgE–R on cells (Figures 3 and 4B, Table III) could have several different causes. It is possible that the formation of IgE–R dimers by the two different monoclonal antibodies A2 and B1E3 reduces the segmental motion of IgE–R on intact cells sufficiently to cause a preferential alignment of the Er emission dipoles along the principal axis of rotation. A dipole moment with a cone angle for wobbling motion of $\leq 20°$ with respect to the principal axis of rotation would be sufficiently restricted to give rise to the results obtained (Kinosita et al., 1984). Although it is quite possible that loss of segmental motion could contribute to the observed loss of phosphorescence anisotropy decay, we think it is unlikely that it could account for the entire effect that is observed on intact cells. As described above, the Er emission dipoles appear to be randomly oriented in several different sites on IgE, so that a decrease of segmental motion would not be sufficient to result in a highly oriented emission dipole. Furthermore, it is not clear why such an increase in dipole alignment would occur on cells but not on membrane vesicles. The similar values of r_0 on cells and vesicles after cross-linking with the anti-IgE antibodies suggest that similar restrictions of submicrosecond motions occur on both cells and vesicles.

It appears likely that the loss of phosphorescence anisotropy decay that is seen with intact cells but not with membrane vesicles is due in large part to interactions with cellular components that dramatically impede the rotational motion of IgE–R in the membrane. Such components could restrict the rotation of IgE–R dimers by interacting at the membrane surface, within the bilayer, or at the cytoplasmic side of the membrane. Qualitatively similar results are obtained with cyclic dimers formed with a bivalent ligand that cross-links via the antibody combining sites (Myers, 1990), indicating that the interactions which result in the apparent loss of rotational motion are not restricted to reagents that cross-link IgE–R via its F_c region. Fluorescence photobleaching recovery experiments on IgE–R dimers made with A2 (Menon et al., 1986b) or B1E3 (Posner, 1991) show a small but significant reduction in the rate of lateral diffusion for these complexes compared with monomeric IgE–R, and this is consistent with a loss of rotational mobility that is implied by the present results.

What is the possible functional significance of a loss of IgE–R rotational mobility upon formation of dimeric complexes on cells? Dimerized IgE–R consistently do not trigger degranulation in RBL cells, but they elicit a transient increase in the concentration of cytoplasmic Ca^{2+} as shown with measurements on single cells with IgE–R dimerized by the bivalent ligand $(DCT)_2$-Cys (Ryan, 1990). Furthermore, addition of $(DCT)_2$-Cys together with the dimer-forming anti-IgE B1E3 causes strong Ca^{2+} mobilization and cellular degranulation, and the magnitudes of these responses are independent of the order of addition or the time interval between additions (Posner, 1991). These results suggest that the formation of the rotationally immobile dimeric complexes "primes" the receptors for the full response that occurs when larger complexes are formed upon addition of a second cross-linking ligand. The results argue against the possibility that the rotationally immobile dimeric IgE–R are desensitized.

What remains to be determined is if the apparent decrease in rotational motion of dimeric IgE–R on intact cells reflects interactions with other cellular components that are directly involved in the activation process. The decrease could also result from more general interactions such as nonspecific molecular entanglements that might occur on cells with ligand-bridged dimers but not with monomeric membrane proteins. In this regard, Damjanovich et al. (1983) measured the rotational mobility of class I MHC molecules on T lymphoma cells in the presence of a monoclonal anti-H-$2K^k$ antibody. The same rotational correlation times were observed with eosin-labeled intact antibody or its Fab fragments, and the addition of a second, noncompeting unlabeled anti-H-$2K^k$ antibody did not cause any reduction in rotational mobility. Further aggregation with a polyclonal antiimmunoglobulin antibody was required for immobilization of the H-$2K^k$ antigen–monoclonal antibody complex. Those data imply that the additional mass of an intact IgG (150 kDa) compared with a Fab fragment (50 kDa) does not cause additional interference to the rotational mobility of a cell-surface membrane protein. It is unclear whether the intact anti-H-$2K^k$ formed dimeric complexes of the class I molecules under the conditions of that experiment, so it is not possible to compare those results to ours in order to assess whether the immobilization we observe with dimeric IgE–R is a special property of IgE–R.

In one recent study, Rahman et al.[2] found that dimers of $Fc_\epsilon RI$ receptors on RBL cells made with eosin-labeled monoclonal antireceptor antibodies in the absence of IgE rotate with a value of ϕ that is about twice that of monomeric receptor. These results suggest that the apparent immobilization of IgE–R dimers that we observe on cells depends on the presence of IgE. We speculate that the interactions causing this immobilization could be involved in reducing the ability of dimeric IgE–R vs dimeric R to trigger cellular degranulation in these cells. In a related study, Pecht et al. (1991) used the same antireceptor antibodies labeled with erythrosin and found more complex anisotropy decay curves that may reflect preferred orientations of the emission dipoles relative to the principal axis of rotation. Future experiments will be aimed at determining the relationship between the changes observed in the present study and receptor function.

Regardless of the cause of the apparent rotational immobilization of dimeric IgE–R on cells, the results imply that signal-transducing components interact with receptors that are undergoing little or no rotational diffusion on the microsecond time scale. Dimeric IgE–R are capable of some lateral movement as measured by fluorescence photobleaching recovery (Menon et al., 1986b; J. Thomas and R. Posner, unpublished results), suggesting that they are not tightly anchored to an immobile structure such as the cytoskeleton. However, more transient interactions with such a matrix, or, alternatively, the formation of a laterally mobile complex with a molecular weight of at least several million, could account for the apparent loss of rotational motion described in the present report. Recent evidence for the activation of tyrosine kinase as an early event in signal transduction stimulated by these $Fc_\epsilon RI$ receptors (Benhamou et al., 1990) points to molecular interactions with other cellular components that are unlike those of the more well-established paradigms for receptor-mediated signal transduction, such as direct receptor–GTP binding protein interactions (Taylor, 1990) or ligand stimulation of an endogenous receptor tyrosine kinase (Yarden &

Ullrich, 1988). It will be necessary to identify the cellular components involved in the IgE–R interactions that lead to signal transduction for complete understanding of how receptor aggregation leads to the activation of a complex cellular response.

ACKNOWLEDGMENTS

We thank Dr. Daniel Conrad for A2 and B1E3 antibodies and Dr. John Hakimi for the purified rat myeloma IR162 IgE.

REFERENCES

Baird, B., & Holowka, D. (1985) *Biochemistry 24*, 6260–6267.
Baird, B., Sajewski, D., & Mazlin, S. (1983) *J. Immunol. Methods 64*, 365–375.
Barsumian, E. L., Isersky, C., Petrino, M. G., & Siraganian, R. (1981) *Eur. J. immunol. 11*, 317–323.
Basciano, L. K., Berenstein, E. H., Kmak, L., & Siraganian, R. P. (1986) *J. Biol. Chem. 261*, 11823–11831.
Beaven, M. A., & Ludowyke, R. (1989) in *Advances in Regulation and Cell Growth* (Mond, J. J., Cambier, J. C., & Wiess, A., Eds.) Vol. 1, pp 245–285, Raven Press, New York.
Benhamou, M., Gutkind, J. S., Robbins, K. C., & Siraganian, R. P. (1990) *Proc. Natl. Acad. Sci. U.S.A. 87*, 5327–5330.
Blank, U., Ra, C., Miller, L., White, K., Metzger, H., & Kinet, J.-P. (1989) *Nature 337*, 187–189.
Cherry, R. J., Nigg, E. A., & Beddard, G. S. (1980) *Proc. Natl. Acad. Sci. U.S.A. 77*, 5899–5903.
Conrad, D. H., Studer, E., Gervasoni, J., & Mohanakumar, T. (1983) *Int. Arch. Allergy Appl. Immunol. 70*, 352–360.
Damjanovich, S., Tron, L., Szollosi, J., Zidovetzki, R., Vaz, W. L. C., Regateiro, F., Arndt-Jovin, D., & Jovin, T. M. (1983) *Proc. Natl. Acad. Sci. U.S.A. 80*, 5985–5989.
Edidin, M. (1987) *Curr. Top. Membr. Transp. 29*, 91–127.
Eisen, H. N., Kern, M., Newton, W. T., & Helmreich, E. (1959) *J. Exp. Med. 110*, 187–196.
Englander, S., Calhoun, D., & Englander, J. (1987) *Anal. Biochem. 161*, 300–306.
Erickson, J. W., Posner, R. G., Goldstein, B., Holowka, D., & Baird, B. (1991) *Biochemistry 30*, 2357–2363.
Fewtrell, C., & Metzger, H. (1980) *J. Immunol. 125*, 701–710.
Garland, P., & Moore, C. (1979) *Biochem. J. 183*, 561–572.
Grassberger, B. (1989) Ph.D. Thesis, University of Maryland, College Park, MD.
Holowka, D., & Metzger, H. (1982) *Mol. Immunol. 19*, 219–227.
Holowka, D., & Baird, B. (1983a) *Biochemistry 22*, 3466–3474.
Holowka, D., & Baird, B. (1983b) *Biochemistry 22*, 3475–3484.
Holowka, D., Conrad, D. H., & Baird, B. (1985) *Biochemistry 24*, 6260–6267.
Holowka, D., Wensel, T., Baird, B., & Stryer, L. (1990) *Biochemistry 29* 4607–4612.
Ishida, N., Ueda, S., Hayashida, H., Miyata, T., & Honjo, T. (1982) *EMBO J. 1*, 1117–1123.
Jovin, T. M., & Vaz, W. L. C. (1989) *Methods Enzymol. 172*, 471–513.
Kawato, S., & Kinosita, K., Jr. (1981) *Biophys. J. 36*, 277–296.
Keegan, A., Fratazzi, C., Shopes, B., Baird, B., & Conrad, D. H. (1991) *Mol. Immunol. 28*, 1149–1154.
Kinosita, K., Jr., Kawato, S., & Ikegami, A. (1984) *Adv. Biophys. 17*, 147–185.
Kulczycki, A., Jr., & Metzger, H. (1974) *J. Exp. Med. 140*, 1676–1695.
Liu, F. T., Bohn, J. W., Ferry, E. L., Yamamoto, H., Molinaro, A. A., Sherman, L. A., Klinman, N. R., & Katz, D. H. (1980) *J. Immunol. 124*, 2728–2736.
Lotan, R., Debray, H., Cacan, M., Cacan, R., & Sharon, N. (1975) *J. Biol. Chem. 250*, 1955–1957.
Menon, A. K., Holowka, D., Webb, W. W., & Baird, B. (1986a) *J. Cell Biol. 102*, 534–540.
Menon, A. K., Holowka, D., Webb, W. W., & Baird, B. (1986b) *J. Cell Biol. 102*, 541–550.
Metzger, H., Alcaraz, G., Hohman, R., Kinet, J.-P., Pribluda, V., & Quarto, R. (1986) *Annu. Rev. Immunol. 4*, 419–470.
Moore, C., Boxer, D., & Garland, P. B. (1979) *FEBS Lett. 108*, 161–166.
Myers, J. N. (1990) Ph.D. Thesis, Cornell University, Ithaca, NY.
Ortega, E., Schweitzer-Stenner, R., & Pecht, I. (1988) *EMBO J. 7*, 4101–4109.
Pecht, I., Ortega, E., & Jovin, T. M. (1991) *Biochemistry 30*, 3450–3458.
Posner, R. (1991) Ph.D. Thesis, Cornell University, Ithaca, NY.
Rigler, R., & Ehrenberg, M. (1973) *Q. Rev. Biophys. 6*, 139–199.
Robertson, D., Holowka, D., & Barid, B. (1986) *J. Immunol. 136*, 4565–4572.
Ryan, T. A. (1990) Ph.D. Thesis, Cornell University, Ithaca, NY.
Saffman, P. G., & Delbruck, M. (1975) *Proc. Natl. Acad. Sci. U.S.A. 72*, 3111–3113.
Segal, D. M., Sharrow, S. O., Jones J. F., & Siraganian, R. P. (1981) *J. Immunol. 126*, 138.
Siraganian, R. P. (1988) in *Inflammation: Basic Principles and Clinical Correlates* (Galling, J. J., Goldstein, I. M., & Snyderman, R., Eds.) pp 513–542, Raven Press, New York.
Taurog, J. D., Fewtrell, C., & Becker, E. L. (1979) *J. Immunol. 122*, 2150–2153.
Taylor, C. W. (1990) *Biochem. J. 272*, 1–13.
Tsuji, A., Kawasaki, K., Ohnishi, S., Merkle, H., & Kusumi, A. (1988) *Biochemistry 27*, 7447–7452.
Velez, M., Barald, K., & Axelrod, D. (1990) *J. Cell Biol. 110*, 2049–2059.
Zidovetzki, R., Bartholdi, M., Arndt-Jovin, D., & Jovin, T. M. (1986) *Biochemistry 25*, 4397–4401.